JOURNAL OF MATERIALS SCIENCE **38** (2003) 4917–4924

Structure and properties of fibrillar silicate/SBR composites by direct blend process

MING TIAN, CHENGDONG QU, YUXING FENG, LIQUN ZHANG*
The Key Laboratory of Beijing City on Preparation and Processing of Novel Polymer Materials, Beijing University of Chemical Technology, Beijing 100029, People's Republic of China
E-mail: tianm@mail.buct.edu.cn

Silicate attapulgite(AT)/Styrene Butadiene rubber (SBR) composites with excellent properties and low cost were first prepared from a direct blending process (including polymer melt blending and emulsion co-coagulation). The structure and properties of above composites were carefully investigated. It was found that most AT separated into dispersed units with diameters less than 100 nm in SBR by the direct blend process. However, a few dispersion units as large as 0.2–0.5 μm and a clear network structure of dispersion units in SBR was observed by TEM, SEM and RPA. AT can be purified, but purified AT cannot be easily dispersed in the rubber matrix by polymer melt blending. Siliane coupling agent Si69 can improve the dispersion of AT and enhance the chemical interfacial adhesion. At the same loading, AT (pretreated with Si69) was found to have better reinforcing effect on SBR than carbon black SRF with particle size 60–100 nm and even than N330 with particle size 26–30 nm to some extent. Meanwhile, the cost of AT/SBR composites is pretty low.

1. Introduction

Polymer nano-composites possess most of the advantages of their matrices. They have light weight, high relative strength (the ratio of strength/density), excellent dielectric properties and can be processed easily. At the same time, due to the introduction of nano-fillers, composites have even higher strength, stiffness and heat resistance compared to their matrix counterparts. In addition, polymer nano-composites also have a series of other unique properties. For example, some polymer nanocomposites are flame-retardant, not permeable to gas and are resistant to UV, bacteria. They also might have excellent magnetic and electronic properties if appropriate fillers are used. Three key issues related to nano-composites are: choosing and/or preparation of suitable nano-fillers; the successful dispersion of the nano-filler; and low cost (at least in mechanical applications). The second issue is very difficult to achieve. From the time that the advantages of polymer nano-composites were first realized, researchers have been seeking nano-fillers of low cost, better dispersibility and excellent reinforcing effects. At the same time, desirable nano-fillers should be able to disperse uniformly in the matrix after simple preparation. This way, the cost of nano-composites would be greatly lowered. It is well known that a kind of inexpensive natural layered silicate (such as montmorillonite and mica) has been widely used together with various polymers to prepare polymer/layered silicate nano-composites [1]. These composites have excellent overall properties and low gas permeability. Major preparation methods of polymer nano-composites include sol-gel [2–4], *in situ* polymerization [5–9] and direct blending (including polymer melt, solution and emulsion blending) methods [10–14]. In recent years, more and more researchers are interested in direct blending because it is the most direct, most cost efficient method and is benign to the environment. Recently, researchers successfully used direct polymer melt intercalation to prepare montmorillonite/nylon6 [11], montmorillonite/poly(epsilon-caprolactone) [12], montmorillonite/PP [13], montmorillonite/EVOH [14] and other polymer nano-composites. In this method, layered silicate must first be organically treated to facilitate its separation and dispersion in the polymer melt.

AT is a type of natural fibrillar silicate clay mineral. There are large reserves of AT in South China (Jiang Su, Zhe Jiang and An Hui province) and in the USA (Florida). AT was first utilized in the 1940s, it has been mainly used as absorbent, catalyst carrier, densifying agent, adhesive and food additive [15]. It is also used as a filler to reduce the cost of polymer materials [16, 17]. In addition, it is used as the nucleation agent for polyoxymethylene (POM) and polypropylene (PP) [18, 19]. There are few reports in the open literature on AT/polymer nano-composites [20, 21], which were prepared by *in situ* polymerization. We found that most AT can be separated into dispersed units with diameters

*Author to whom all correspondence should be addressed.

less than 100 nm in polymer with high viscosity through polymer melt blending. A few large dispersion units as large as 0.2–0.5 μm were also observed. A clear network structure of dispersion units was formed. AT can be purified, but purified AT cannot be easily dispersed by polymer melt blending. Silane coupling agent Si69 can enhance the chemical interfacial adhesion between AT and SBR, in addition, it can improve the dispersion of AT in SBR. AT/SBR nano-composites prepared from polymer melt blending have excellent properties.

2. Experimental

2.1. Materials

AT was provided by Jiangsu AT Co. Ltd., China. It was sieved by 325 mesh sieve. SBR1500 was provided by Qi Lu Petroleum Company, China. NaA, polyacrylate sodium, has a molecular weight of 4000–6000. PAA, maleic acid anydride and acrylate sodium copolymer, has a molecular weight of 4000–6000, Shenyang Xinqi Co. Ltd., China. Si69, Bis-(3-thiethoxy silylpropyl)-tetrasulfide $(C_2H_5O)_3Si(CH_2)_3S_4(CH_2)_3Si(OC_2H_5)_3$ and other chemical agents were common chemicals.

2.2. Preparation of composites

2.2.1. Polymer melt blend method from polymer melts

SBR was put into the two-roll mill first, adjusting the two rolls to the smallest distance when SBR became fluid. AT was then slowly added into SBR to ensure good dispersion. Active agent, accelerator and antioxidant were added thereafter (see Table I). The cross-linking time at 150°C was determined from an oscillating disc rheometer. Test specimens were then prepared from the vulcanized material.

2.2.2. Polymer emulsion co-coagulation method

AT was dispersed in water first and then mixed with SBR emulsion. $CaCl_2$ solution was then added into the mixture after it was stirred for 1.5–2.0 h. Deposited material was then dried in a vacuum oven at 50°C for 24 h and a dry compound consisting of SBR and dispersed AT was obtained. Additives were added as described above and the final compound was vulcanized. Test specimens were then prepared from the vulcanized material.

TABLE I Compositions of materials

Styrene butadiene rubber	100
Zinc oxide	5.0
Staeric acid	2.0
Accelerator D	0.5
Accelerator DM	0.5
Accelerator TT	0.2
Sulfur	1.75
Antioxidant 4010NA	1.0
Filler	Variable

Accelerator D: diphenyl guanidine, Accelerator DM: dibenzothiazole disulfide, and Accelerator TT: tetramethyl thiuram disulfide.

2.2.3. Characterization

Tensile tests were carried out according to Chinese standard GB/T 528-92 using an Instron tensile machine. The crosshead speed was set as 500 mm/min in all experiments. Tear strength and hardness of composites were measured according to Chinese standard GB/T 529-91 and GB/T 531-92 respectively.

Transmission Electron Microscope (TEM) was used to study the morphology of the composites. A H-800 TEM was used to observe the thin section cut from the sample by microtome at −100°C. The acceleration voltage was 200 kV. Cryo-fracture surfaces of nano-composites were observed under a S-250MK3 Scanning Electron Microscope (SEM) from CAMBRIDGE.

The specific surface area (Nitrogen adsorbate) of AT was determined by Quantachrome Autosorb Gas Sorption System from Quantachrome Corporation in US.

X-ray diffraction (XRD) patterns were obtained with a Rigaku RINT X-ray diffractometer using Ni-filtered Cu K_α radiation, a 0.02° step size, and 6.00°, 2θ/min.

The Payne effect of the AT/SBR compound was investigated by RPA 2000 from Monsanto Company at 60°C, and test frequency 1 Hz.

3. Results and discussion

3.1. Structure and properties of AT

The chemical structure of AT is $Mg_5[Al]Si_8O_{20}(HO)_2$-$(OH_2)_4 \cdot 4H_2O$. Its structure is illustrated in Fig. 1. Its microstructure can be classified into three levels. Fibrillar single crystal is the smallest structure unit with a length of 500–2000 nm and 10–25 nm in diameter (Fig. 2a, structure level 1). Each single crystal consists of many unit layers. Each unit layer consists of two silicone and oxygen tetrahedrons. In between adjacent unit layers are five aluminium-oxygen tetrahedrons. Unit layers are connected by oxygen atoms and formed a tunnel like crystal structure. Single crystals are compactly arranged in parallel and formed crystal bundles (Fig. 2a, structure level 2). These crystal bundles are then agglomerated into micro-scale AT particles (Fig. 2b and c, structure level 3). There is a lot of hydroxysilicone on the surface of AT single crystals. Interaction between single crystals are mainly Van der Waals forces and hydrogen bonds [22, 23]. It is important that the interaction between single crystals is much smaller than that between layers in layered silicates. Unlike the layer-layer interaction existing in layered silicates, the

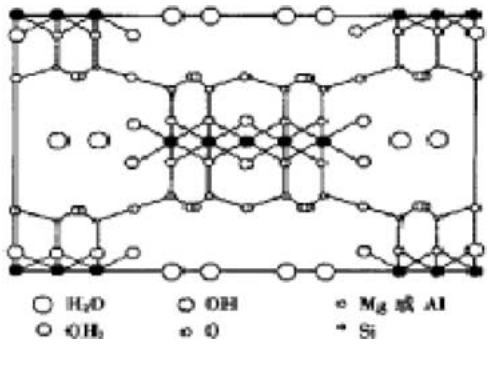

Figure 1 Structure of attapulgite crystal.

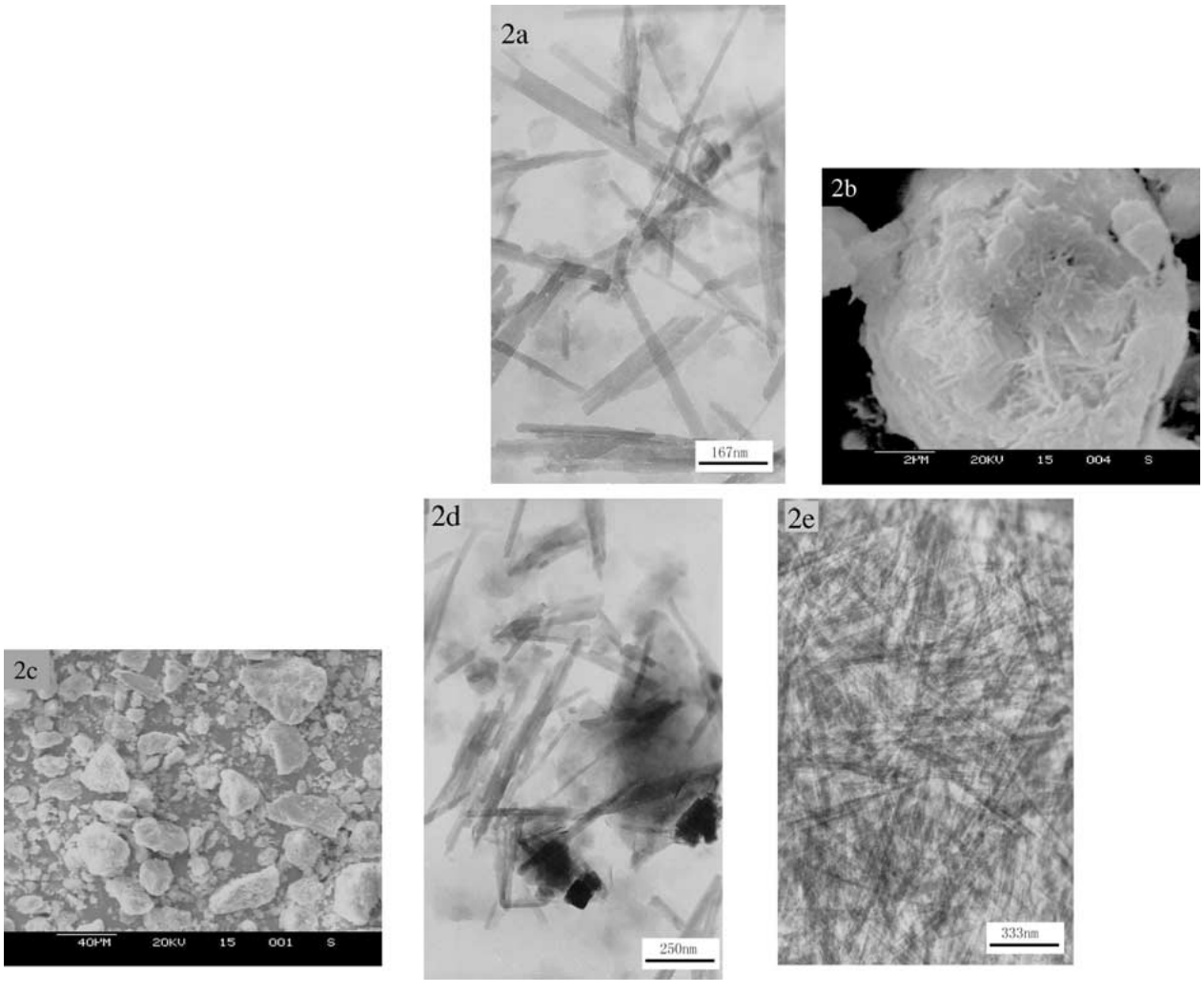

Figure 2 Morphology of AT (a, b: Unpurified AT; c, d: Unpurified AT in water; e: Purified AT in water).

interaction area between AT single crystals is extremely small due to a similar line-line contact, which results in a weak interaction. Furthermore, there are a lot of interstice spaces between these geometrically agglomerated nano-scale single crystals. These characteristics will facilitate the decohesion (separation) of AT micro-agglomerates into smaller scale crystal bundles and single crystals upon large shear or physical and chemical modification.

Unpurified AT has some other composition besides AT, such as quartz and carbonate [15]. These chemicals exist in the form of relatively large particles (Fig. 2d), which are difficult to be dispersed in water or separated under shear into smaller dispersion units. These large particles in the matrix will deteriorate the mechanical properties of rubber, thus we tried to purify AT. From Table II, it can be seen that the dispersion agent and stir rate do not affect the yield of AT much, AT yield is 65–67%, this value is consistent with that reported in the literature [15]. NaA and PAA can effectively improve the purification of AT, purified AT has a narrower diameter distribution (Fig. 2e); at the same time, large AT crystal bundles or agglomerates were decohered into numerous small crystal bundles or single crystals under the dual effects of water and strong shear.

3.2. Morphology of unpurified AT/SBR composites from polymer melt blend

After unpurified AT and SBR were directly blended on the two-roll mill, most AT particles were decohered and dispersed as fibrillar single crystals or crystal bundles with a diameter smaller than 100 nm under mechanical shear, refer to the shallow dark domain in Fig. 3a. This further demonstrated that interaction between AT single crystals is much weaker than that between the layers of layered silicates. It is well known that layered silicates cannot be directly separated into nano-units to disperse in rubber by direct blending [24, 25]. However, these fibrillar single crystals or crystal bundles were broken also under shear and became shorter. Still, some particles as large as 0.2–0.5 μm (darker domain in

TABLE II Effect of purification condition on AT yield

	Purification condition		
AT production site	Dispersing agent	Stir rate	AT yield (%)
Jiang Su	NaA	3980 r/min	67.06
Jiang Su	NaA	800 r/min	65.07
Jiang Su	PAA	3980 r/min	65.37

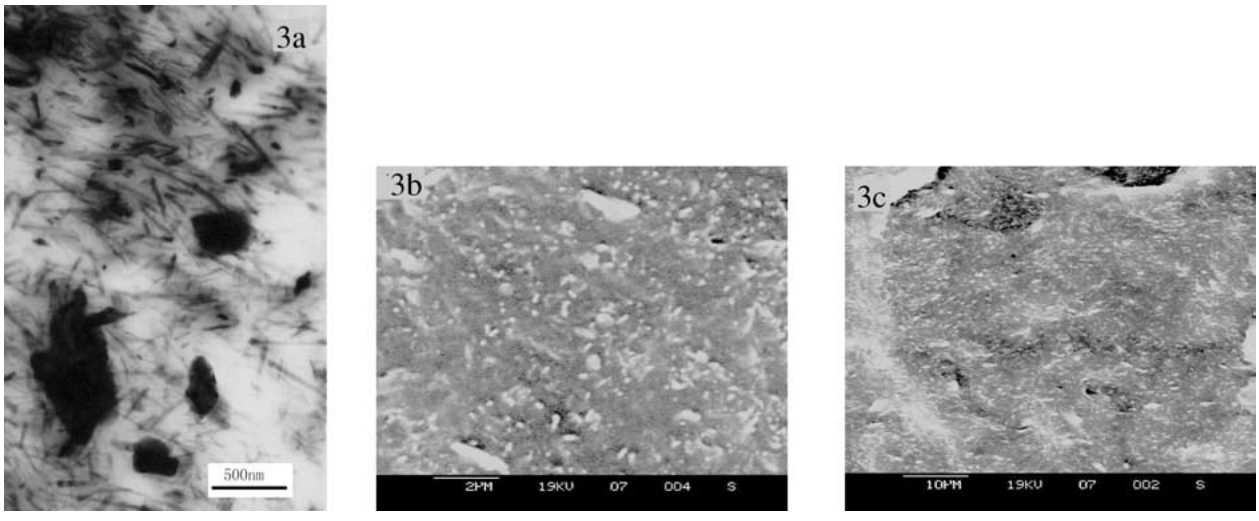

Figure 3 Morphology of unpurified AT/SBR composites from polymer melt blend.

Fig. 3a and b) were observed by TEM and SEM, they are much smaller than the original particles in unpurified AT (Fig. 2a). This indicates that these smaller particles may be impurities in AT and unseparated AT, and/or AT whose interaction between crystals is very strong. Furthermore, the smooth and clear fracture surface of the composites indicates that the interfacial adhesion between AT and the rubber matrix is not strong enough (Fig. 3c).

3.3. Morphology of purified AT/SBR composites from polymer melt blend

After AT was purified by NaA and dried with a spray drier, it was blended with SBR directly to make purified AT/SBR composites. Although some AT dispersed as small dispersion units, most AT remained as large particles (outlined by the dark edges in Fig. 4a) in SBR. This is because purified AT was driven by thermodynamic force to re-agglomerate into a fibrillous network structure during drying process. This is a more compact structure compared to unpurified AT and is difficult to be dispersed in SBR matrix directly. It is not a desired result.

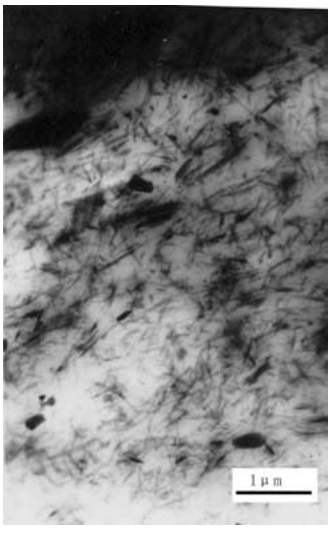

Figure 4 Morphology of purified AT/SBR composites from polymer melt blend.

3.4. Morphology of AT/SBR composites from emulsion co-coagulation method

Compared to the direct blending method, the co-coagulation method can improve the dispersion of AT in SBR (Fig. 5). The basic principle of co-coagulation method is that AT (including purified AT) can be easily separated into single crystal-nanofibers in water, then nanofibers were surrounded by latex particles added subsequently, finally salt solution was added into the mixture, and the nanofibers and rubber latex were co-coagulated together. AT fibers are short from NaA purification and dispersed very uniformly in the matrix (Fig. 5a). AT fibers are relatively long after PAA purification, but the dispersion is less uniform (Fig. 5b). The dispersion of unpurified AT is the worst among three (Fig. 5c) from the viewpoint of existence of unseparated impurities, but better than that of unpurified AT/SBR composites from polymer melt blending (Fig. 3a). Nevertheless, some small AT agglomerates were observed in composites from all of the above three routes. The thickness of most of Agglomerates of purified AT in SBR is about 0.2 μm, which was relatively small (Fig. 5d and e). This can be explained by the effect of NaA and PAA. NaA and PAA not only removed the impurities in AT, but also increased the viscosity of the emulsion and dispersion of AT in the emulsion. Therefore, purified AT was relatively stable in the emulsion. AT would not deposit and re-agglomerate due to gravity, but was surrounded and separated by SBR latex particles. Therefore, AT was dispersed uniformly in the SBR matrix after co-coagulation in finer units. Unpurified AT tends to deposit in the emulsion due to gravity, also ion like Ca^{2+} introduced by impurities lowers the stability of the emulsion (flocculation effect). Thus, AT was not uniformly dispersed in the emulsion. At the same time, impurities were brought into and existed in large sizes in the polymer matrix. Therefore, purified AT produced better composites from the co-coagulation method.

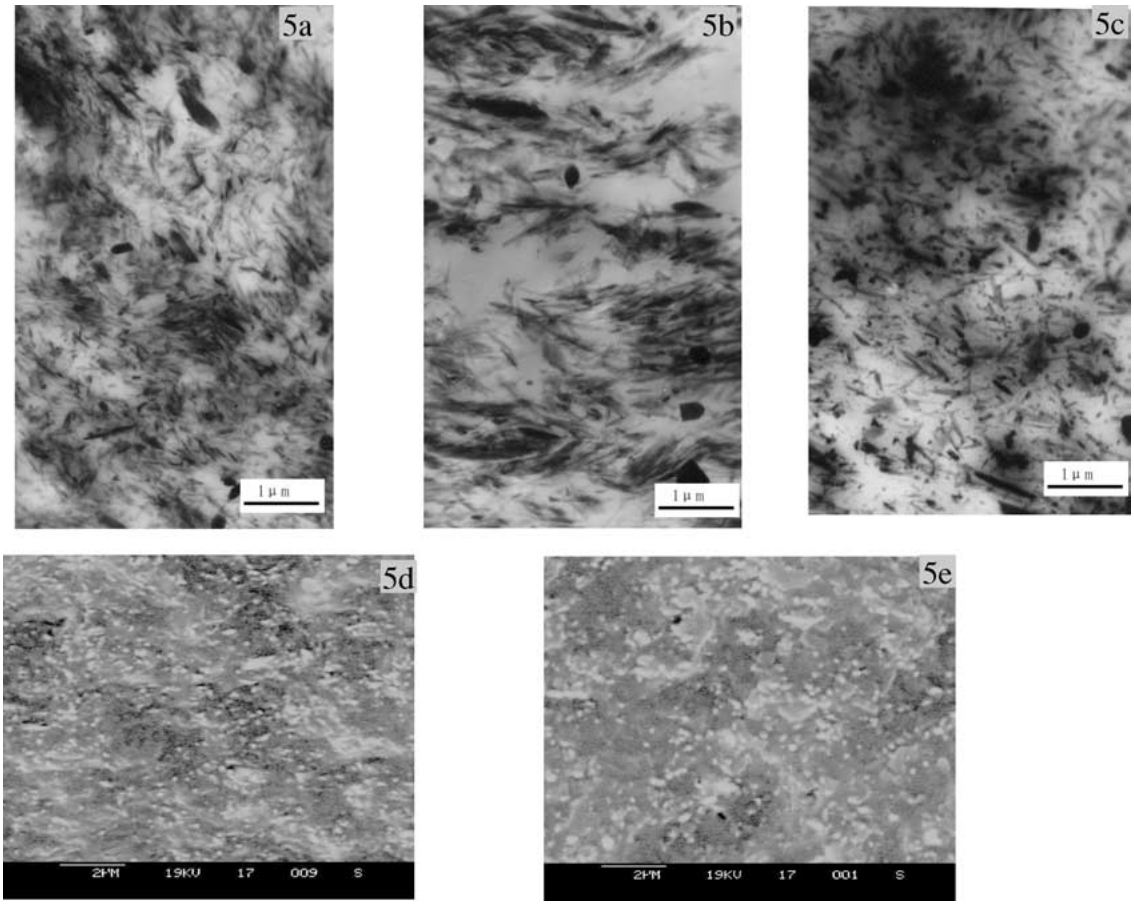

Figure 5 Morphology of AT/SBR composites from emulsion co-coagulation method. a, d: NaA purified AT; b, e: PAA purified AT; c: unpurified AT.

3.5. Morphology of unpurified AT/Si69/SBR composites from direct melt blend

Fig. 6 showed that AT could disperse in the SBR matrix more uniformly after the addition of Si69. This is due to the fact that Si69 was coated on the surface of AT, the active ethoxy group of Si69 will react with the silicone hydroxy group on AT. The organic components introduced on the surface of AT decreased the agglomeration of AT and further improved the dispersion of AT in the SBR matrix (Fig. 6a and b). At the same time, the sulfur atom in Si69 will participate in the vulcanizing reaction of SBR and enhance the interfacial adhesion between AT and SBR matrix. The fracture surface of the AT/Si69/SBR composite in Fig. 6c showed less clear morphology compared with AT/SBR (Fig. 3c).

3.6. X-ray diffraction patterns of AT/SBR composites

Fig. 7 gives the X-ray diffraction patterns of AT and AT/SBR composites. Both AT and AT/SBR composites, a characteristic peak appears at 8.34°, which

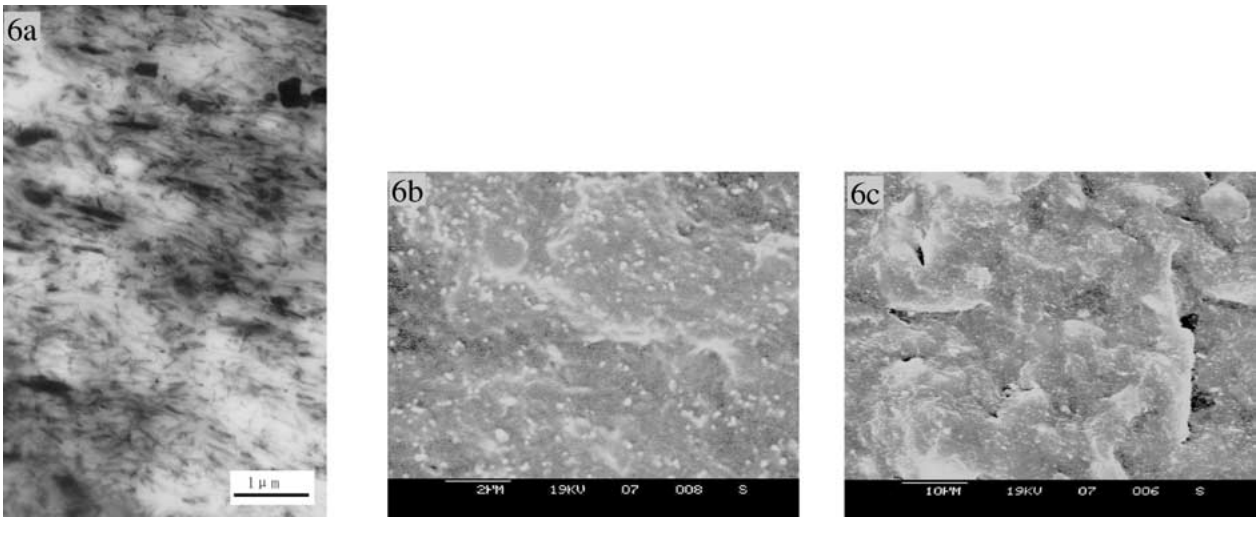

Figure 6 Morphology of AT/Si69/SBR composites from polymer melt blend method.

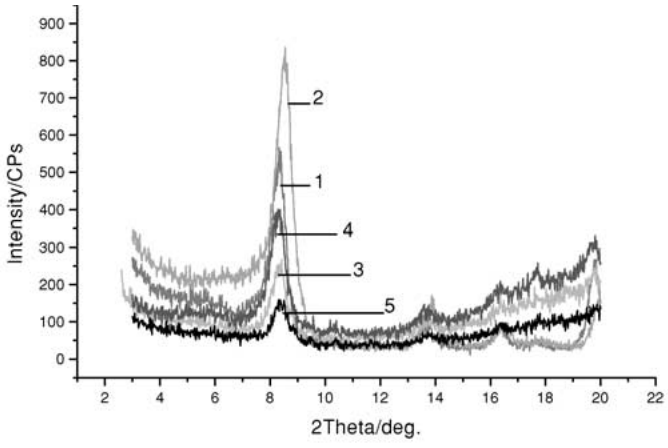

Figure 7 X-ray diffraction patterns of AT/SBR composites: 1, unpurified AT; 2, purified AT; 3, purified AT/SBR composites by emulsion co-coagulation; 4, unpurified AT/SBR composites by melt blend; 5, AT/Si69/SBR composites by melt blend.

corresponds to 1.05 nm layer distance. It is reported that sepiolite as well as AT is composed of crystals consisting of unit layers and layer distance between single crystals is 1.2 nm [26], therefore, the layer distance in Fig. 7 is not between AT single crystals, but between unit layers in single crystal. Unit layers in a single crystal cannot further be separated, therefore the position of this characteristic peak was not changed when AT was separated. However, the intensity of this characteristic peak can be used to identify the separation of AT to some extent. Compared with AT, the characteristic peaks of AT/SBR composites become attenuated because of the decrease of concentration of AT. Similarly, the peak intensity of X-ray diffraction of purified AT is higher than that of raw AT. When the co-coagulating method was applied or siliane coupling agent was introduced, the dispersion (i.e., separation) of AT in SBR was improved greatly as discussed before, which lowered the X-ray diffraction probably because of separation, disorder of AT single crystals in the matrix.

3.7. Properties of AT/SBR composites

From Table III, it can be seen that unpurified AT improved the mechanical properties of SBR from polymer melt blends. Hardness, 300% tensile stress, tensile strength, tear strength, elongation at break and tensile set of AT/SBR composites all increased with increasing AT content. As described before, AT can be decohered into single crystals or crystal bundles by mechanical shear and still keep a relatively high aspect ratio. Therefore, AT showed pronounced reinforcing effect. At the same time, AT micro-agglomerates will break up during tensile process, which will increase elongation at break and tensile set.

From Table IV, it can be seen that the mechanical properties of purified AT/SBR were not as good as unpurified AT/SBR, which were both prepared by polymer melt blending. This to say, purification did not increase mechanical properties of the composites as expected, purification even decreased properties of the AT/SBR properties. This is because the dispersion of purified AT/SBR is less uniform. This is consistent with the morphology observed before.

Compared with unpurified AT/SBR composites from polymer melt blends, AT/SBR composites from the emulsion co-coagulation method have even better mechanical properties (see Table V). AT purified by PAA

TABLE III Effect of the amount of unpurified AT on mechanical properties of composites by polymer melt blend

Content of filler (g/100 gSBR)	10	20	30	40	50	60
Shore A hardness	48	52	54	56	60	62
300% tensile stress (MPa)	1.5	1.9	2.1	2.1	2.5	3.2
Tensile strength (MPa)	2.3	3.5	4.7	7.6	7.4	9.1
Elongation at break (%)	468	632	728	900	848	904
Tensile set (%)	4	12	24	52	60	64
Tear strength ($kN \cdot m^{-1}$)	18.6	18.3	21.3	22.2	30.5	37.3

TABLE IV Effect of purification of AT on mechanical properties of composites by polymer melt blend

Properties	Unpurified AT	Purified AT by NaA
Shore A hardness	56	56
300% tensile stress (MPa)	2.1	1.9
Tensile strength (MPa)	7.6	6.1
Elongation at break (%)	900	972
Tensile set (%)	52	48
Tear strength ($kN \cdot m^{-1}$)	22.2	21.7

40 gAT/100 gSBR.

TABLE V Effect of the purification way of AT on mechanical properties of composites by co-coagulation

Properties	Unpurified AT	PAA purification	NaA purification
Shore A hardness	66	66	66
300% tensile stress (MPa)	2.8	3.0	2.6
Tensile strength (MPa)	9.2	9.6	11.8
Elongation at break (%)	884	892	804
Tensile set (%)	52	80	60
Tear strength ($kN \cdot m^{-1}$)	33.0	30.4	30.8

40 gAT/100 gSBR.

TABLE VI Effect of the amount of Si69 on mechanical properties of composites by polymer melt blend

Content of modifier (w/40 gAT)	0	0.5	1	2	4	6	7	10
Shore A hardness	56	62	62	64	68	70	70	72
300% tensile stress (MPa)	2.1	3.2	4.0	4.9	9.9	11.1	9.3	9.6
Tensile strength (MPa)	7.6	10.9	11.7	13.5	13.6	14.8	14.4	14.3
Elongation at break (%)	900	888	856	776	552	456	584	548
Tensile set (%)	52	40	38	30	18	14	14	12
Tear strength ($kN \cdot m^{-1}$)	22.2	38.7	46.5	55.7	66.7	68.7	67.9	70.6

has about the same reinforcing effect on SBR as unpurified AT, while AT purified by NaA has a better reinforcing effect compared to unpurified AT (see Table V). This is also consistent with previous morphology observation.

3.8. Properities of unpurified AT/Si69/SBR composties

Table VI indicates that Si69 significantly improved the mechanical properties of AT/SBR. Within a certain range, the hardness, 300% tensile stress, tensile strength and the tear strength of the composites significantly increased with increasing Si69 content. The elongation at break and tensile set decreased with increasing Si69 content. The optimum content of Si69 is determined to be 15% (i.e., 6 g additive/40 g AT). The mechanical properties of AT/SBR did not change much if the Si69 content passed this optimum content. The mechanical properties of AT/Si69/SBR composites are better than those of SRF/SBR, noteworthy here is that AT/Si69/SBR composites have very high tear strength. This further supported the argument that addition of Si69 improved the reinforcing effect.

From Table VII, except the larger tensile set, all AT/Si69/SBR composites have better mechanical properties than SRF/SBR and even N330/SBR composites under the same mass content (in fact, AT has a smaller volume content). Noteworthy here is that AT/Si69/SBR composites have higher 300% tensile stress and tear strength. Surprisingly, unpurified AT has a better reinforcing effect than purified AT after pretreatment of Si69. We find that the specific surface area of purified AT is 147.8 m^2/g, lower than value of unpurified AT, 171.3 m^2/g. This seems to be consistent with the fact of close packing of purified AT, and also because purification impairs the interaction between AT surface and Si69 due to occupation of NaA or PAA on the surface of AT crystal. The reason why the properties of composites from polymer melt blending are also higher than those of composites from the emulsion preparation is that after processing Si69 pretreated AT is not easy to disperse into SBR emulsion due to the organic characteristic of the surface.

TABLE VII Mechanical properties of SBR composites

Properties	1	2	3	4	5*
Shore A hardness	70	68	72	58	62
300% tensile stress (MPa)	11.1	9.8	8.8	6.0	7.4
Tensile strength (MPa)	14.8	12.9	13.8	6.9	19.4
Elongation at break (%)	456	464	620	360	488
Tensile set (%)	14	12	36	2	4
Tear strength ($kN \cdot m^{-1}$)	68.7	45.4	48.3	26.3	35.2

40 gAT/100 gSBR; *the same volume as AT: 1, unpurified AT+15%Si69, by polymer melt blend; 2, unpurified AT+15%Si69 by emulsion co-coagulation; 3, PAA purified AT+15%Si69, by emulsion co-coagulation; 4, SRF, particle size 60–100 nm; 5, N330, particle size 26–30 nm.

3.9. Payne effect of AT/SBR compound

The Payne effect is directly related to the network structure formed by filler in a polymer matrix, hence it is often used to characterize the three-dimensional distribution of filler [27–30]. The filler network will be destroyed under a higher strain. As a result, the dynamic modulus (G') will rapidly be lowered. The lower is the attenuation of dynamic modulus, the lower is the filler network structure, and the weaker is the Payne effect. This indicates that the filler in the polymer may be dispersed more uniformly. Seen from Fig. 8a, among three AT/SBR compounds, the Payne effect in AT/Si69/SBR compound from direct melt blending is the weakest, while the Payne effect in the AT/SBR compound from

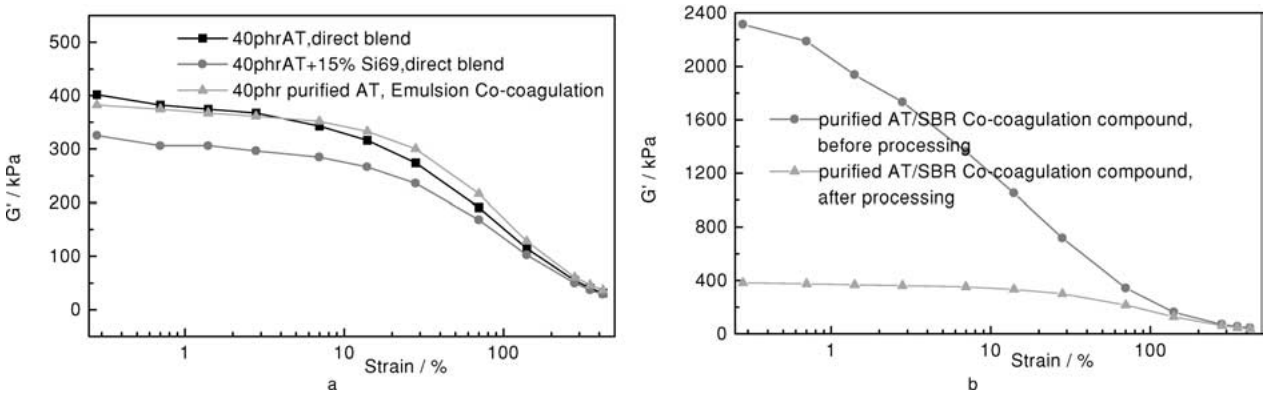

Figure 8 Payne effect of AT/SBR compound.

polymer melt blending is the strongest. This implies that AT in AT/Si69/SBR compound disperses most uniformly resulting in a low filler network structure and dynamic modulus, therefore the modulus attenuation due to the collapse of the filler network structure is the lowest. This agrees with the explanation and the morphology observed before.

From Fig. 8b, after processing, AT/SBR co-coagulation mixture has much lower dynamic modulus than that of unprocessed AT/SBR coagulation compound; the same is true of the attenuation of dynamic modulus. This is the fact, which has been seen from the TEM morphology before (Figs 2e and 5a), that the length of AT nanofibers before processing is much longer than that of AT after processing. Apparently, the longer dispersion phase more easily constructs the filler network in matrix.

4. Conclusions

Relatively strong polar dispersing molecule (such as water and PAA solution) can easily diffuse into the interstices in-between nano-crystals. This will facilitate decohesion of AT into nano-crystals. Si69 can react with the active functional groups on the surface of single AT crystals and facilitate the separation of AT in the polymer blending process, and improve the interaction between rubber and AT. In SBR, most AT can be decohered into nanometer scale single crystals or crystal bundles without any additional treatment.

Because AT can be relatively easily separated into single crystals and crystal bundles, a type of new low cost polymer micro and nano-composite with excellent overall properties can be obtained from conventional polymer melt blending or emulsion co-coagulation. The properties of the composites were determined by the dispersion and interfacial adhesion between filler and polymer matrix.

Acknowledgements

The authors thank Ministry of Science and Technology of China for capitals as well as Committee of National Nature Science Fund of China. Supported by 863 High Technology Research Plan of China (2002AA334050) and National Nature Science Fund of China (05173003).

References

1. Y. P. WU, L. LIU, D. S. YU and L. Q. ZHANG, *J. China Synthetic Rubber Industry* **25**(2) (2002) 65.
2. Y. H. ZHANG and K. C. GONG, *J. Polym. Mater. Sci. Eng. (China)* **13**(4) (1997) 14.
3. J. H. SUN, Y. ZHANG and W. H. FAN, *J. Prog. in Chem.* **11**(1) (1999) 80.
4. J. F. ZHANG, Q. ZHENG, C. Y. GAO and X. F. YI, *J. Functional Materials* **16**(5) (2000) 5.
5. Y. FUKUNSHIMA, A OKADA and M. KAWASUMI, *J. Clay Miner.* **23** (1998) 27.
6. Y. C. KE, C. F. LONG and Z. N. QI, *J. Appl. Polym. Sci.* **71** (1999) 1139.
7. S. G. LYU, G. R. PARK and G. S. SUR, *J. Polymer (Korea)* **23**(6) (1999) 884.
8. J. G. DOH and I. CHO, *J. Polymer Bulletin* **41** (1998) 511.
9. J. HEINEMANN, H. REICHERT, R. THOMANN and R. MUELHAUPT, *Macromol. Rap. Commun.* (8) (1999) 423.
10. L. Q. ZHANG, Y. Z. WANG, D. S. YU, Y. Q. WANG and Z. F. SUN, CN98101496.8, 1998, China.
11. L. M. LIU, Z. N. QI and X. G. ZHU, *J. Appl. Polym. Sci.* **71**(7) (1999) 1133.
12. H. K. CHOI, Y. H. PARK and S. G. LYU, *J. Polymer (Korea)* **23**(5) (1999) 724.
13. N. HASEGAWA, M. KAWASUMI, M. KATO, USUKI ARIMITSU and OKADA AKANE, *J. Appl. Polym. Sci.* (67) (1998) 87.
14. N. ARTZI, Y. NIR, D. WANG and M. NARKIS, *J. Polym. Comp.* **22**(5) (2001) 710.
15. S. H. YAN, Clay Miner. (Beijing Publisher, Beijing, 1981).
16. S. C. J. PENG, *Nonmental Miner. (China)* **1** (1998) 15.
17. Z. SHENG, C. Y. CHU, C. S. SHAO and H. XU, *J. Chemistry Engineer (China)* **2** (1996) 3.
18. W. B. XU and P. S. HE, *J. Appl. Polym. Sci.* **80**(2) (2001) 304.
19. A. SHU, P. CUI and F. Y. WEI, *J. Anhui Chem. Industry(China)* (**2**) (1997) 34.
20. Y. Z. WANG, H. DONG and D. S. YU, *J. Synthetic Resin & Plastics (China)* **14**(2) (1997) 16.
21. J. F. RONG, Z. H. JING, X. Y. HONG and W. ZHANG, CN98125042 (Appl), 1998.
22. J. GU, N. LIU, Y. LI and Y. J. MA, *J. Silicate (China)* **6** (1999) 50.
23. Y. S. FANG, J. Q. XU and L. W. LI, *J. Nanjing Univ. (China)* **1** (1990) 15.
24. L. Q. ZHANG, Y. Q. WANG, Y. Z. WANG, Y. P. WU, H. F. ZHANG and J. Y. HE, *J. Beijing Univ. Chem. Tech. (China)* **27**(2) (2000) 10.
25. ZILG CARSTEN, THOMANN RALF, MÜLHAUPT ROLF and FINTER JÜRGEN, *Adv. Mater.* **11**(1) (1999) 49.
26. YUMIN HE, *Jiangsu Geology (China)* **1** (1986) 29.
27. G. GEORG, A. BOHM and N. NGUYEN, *J. Appl. Polym. Sci.* **55** (1995) 1041.
28. G. WU, S. ASAI, M. SUMITA, R. HIGUCHI and J. WASHIYAMA *Coll. Polym. Sci.* **278** (2000) 220.
29. M. KLUPPEL and R. H. SCHUSTER, *Rubber Chem. Technol.* **70** (1997) 243.
30. K. MIYASAKA, K. WATANABE, E. JOJIMA, HIROMI AIDA, MASAO SUMITA and KINZO ISHIKAMA, *J. Mater. Sci.* **17** (1982) 1610.

Received 18 November 2002
and accepted 27 August 2003